

EFFECT OF REAGENT ROTATIONAL ENERGY ON PRODUCT-STATE DISTRIBUTION IN THE REACTION $\text{Ca} + \text{HF} \rightarrow \text{CaF} + \text{H}$

R. ALTKORN*, F.E. BARTOSZEK**, J. DEHAVEN, G. HANCOCK ‡, D.S. PERRY ‡
and R.N. ZARE ‡

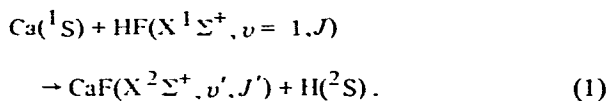
Department of Chemistry, Stanford University, Stanford, California 94305, USA

Received 15 April 1983; in final form 31 May 1983

The effect of reagent rotation on the product vibrational state distribution is reported for the reaction $\text{Ca}(^1\text{S}) + \text{HF}(X^1\Sigma^+, v=1, J) \rightarrow \text{CaF}(X^2\Sigma^+, v', J') + \text{H}(^2\text{S})$. An infrared optical parametric oscillator selects $\text{HF}(v=1)$ in each of its first eight rotational levels. As reagent rotational energy is increased, new product vibrational levels appear whose populations appear to be described by a statistical distribution.

1. Introduction

In this letter we report preliminary results concerning the dynamics of the chemical reaction



An optical parametric oscillator (OPO) prepares the HF molecule in a selected rotational level, $J=0-7$, of the $v=1$ state. A visible dye laser probes the resulting CaF product to determine its nascent internal-state distribution from its fluorescence excitation spectrum. We find that reagent rotation is efficiently converted to product vibration.

For some time, tunable dye lasers have been used to examine product internal-energy distributions in reaction dynamics experiments [1]. The use of lasers

in reagent vibration-rotation state preparation, however, has in general been limited to cases in which molecular absorption features either overlap fortuitously with fixed-frequency sources or are accessible by excitation with chemical lasers [2,3]. The lithium niobate OPO used in this experiment is a powerful source of pulsed coherent infrared radiation, tunable from 1.4 to 4.4 μm [4]. It is an attractive instrument for reagent state preparation, capable of extending the range of molecular systems whose state-to-state reaction dynamics can be studied, and, in the present case, permits the preparation of $\text{HF}(v=1, J)$ in rotational states outside the practical range of the HF laser.

2. Experimental

The apparatus will be described in detail in a future publication and only the immediately relevant characteristics are outlined here. A thermal beam of Ca atoms traverses HF gas at low density. The output beams from the OPO (pump) and from an N_2 -laser-pumped dye laser (probe) counterpropagate along an axis perpendicular to the calcium beam. Laser-induced fluorescence (LIF) is detected along the third orthogonal axis by a photomultiplier tube (RCA 7265). The signal is processed by a boxcar averager (PAR 164/162) and a signal averager (Nicolet 1172). The signal averager per-

* NASA training grant recipient, 180-82.

** Present address: Ontario Hydro, Science Section, 800 Kipling Avenue, Toronto, Ontario, Canada M8Z 5S4.

‡ Present address: Physical Chemistry Laboratory, Oxford University, South Parks Road, Oxford OX1 3QZ, UK.

‡ Present address: Department of Chemistry, University of Rochester, River Station, Rochester, New York 14637, USA.

‡ Holder of a Shell Distinguished Chair, funded by the Shell Companies Foundation, Inc.

mits a point-by-point subtraction of the LIF resulting from background CaF formed in the oven chamber.

The OPO consists of an angle-tuned LiNbO₃ crystal pumped by a Nd : YAG laser*. A grating and etalon inside the resonant cavity narrow the linewidth (<0.5 cm⁻¹). An opto-acoustic cell is used to tune the OPO to individual absorption lines and to monitor the long-term stability of the output power which is typically ±10%. Excitation of HF(*v* = 1, *J*) is accomplished via R-branch lines except for *J* = 0 in which case the P(1) line is used.

The spectra reported in this paper are the result of several (4–33) repetitive scans of the dye laser and have been smoothed by adding together adjacent channels of the signal averager within the limits set by the

* The LiNbO₃ crystal, measuring 6 cm long by 1.5 cm in diameter, was fabricated by the Center for Materials Research, Stanford University. After roughly 10⁸ shots, it continues to oscillate, with grating and intracavity etalon, at conversion efficiencies ranging from 5% to 12%.

Table 1
Values of experimental parameters

HF pressure	2×10^{-4} Torr
oven temperature	1100 K
Ca atom flux	1.3×10^{16} cm ⁻² s ⁻¹
probe-laser energy	8–12 μJ/pulse
probe-laser bandwidth	0.3–0.4 cm ⁻¹
probe-laser spot size	0.5 cm diameter
probe-laser polarization ^{a)}	0.9
OPO energy (idler)	3–5 mJ/pulse
OPO bandwidth	<0.5 cm ⁻¹
OPO spot size	0.6 × 1 cm
OPO polarization ^{a)}	-0.7
pump-probe delay	13 μs
boxcar gatewidth	50 ns ^{b)}

a) Polarization is $(I_1 - I_2)/(I_1 + I_2)$ where I_1 and I_2 are the laser intensities corresponding to alignment of the electric vector of the laser parallel and perpendicular to the calcium atom beam, respectively.

b) The lifetime of CaF($A^2\Pi_{1/2}$) is 21.9 ± 4 ns [5].

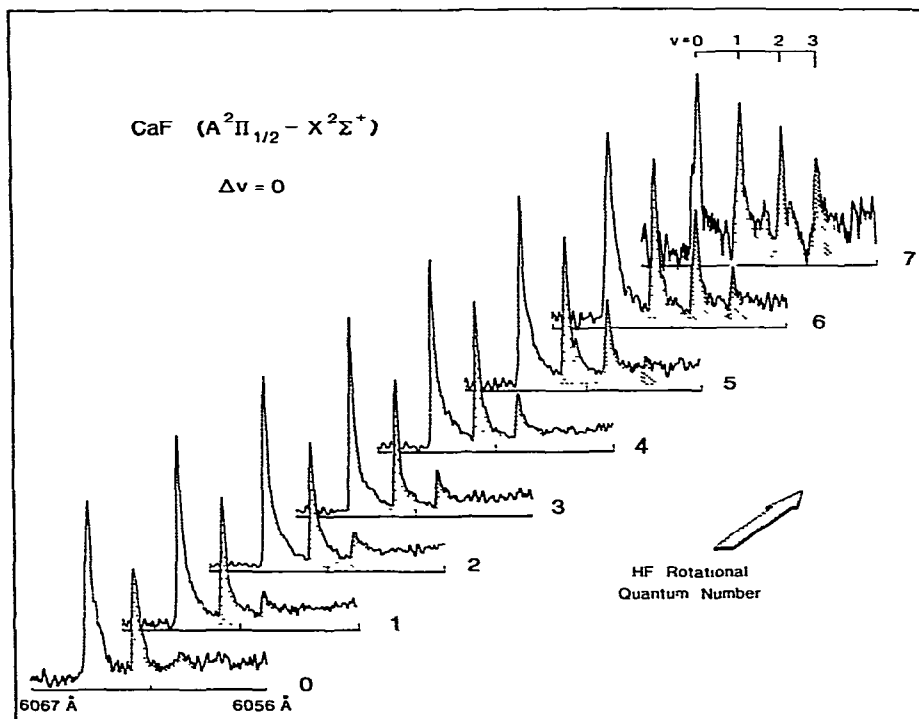


Fig. 1. Laser-excitation spectra of CaF($A^2\Pi_{1/2} - X^2\Sigma^+$) formed in the Ca + HF($X^1\Sigma^+$, $v = 1, J$) reaction, as a function of HF rotational quantum number *J*. Bandheads corresponding to individual CaF vibrational levels are shaded differently to facilitate visual comparison between spectra.

dye-laser bandwidth. They are obtained under identical conditions of oven temperature, HF pressure, probe-laser bandwidth, laser power, etc. These conditions are summarized in table 1.

3. Results

The LIF excitation spectra for $\text{CaF}(A^2\Pi_{1/2}-X^2\Sigma^+)$ as a function of $\text{HF}(v=1)$ rotational energy are shown in fig. 1. Each spectrum is normalized to the height of the (0,0) bandhead. Within the limits of experimental error (table 2), the relative intensities of the bandheads remain unchanged with the reduction of up to a factor of 100 in probe-laser power (the lowest laser power being determined by an acceptable signal-to-noise ratio). These features are also found to be independent of HF pressure (uncorrected ionization gauge readings

of 4×10^{-5} – 8×10^{-4} Torr), pump-probe delay, number of scans, the use of smoothing routines, and polarization of the probe laser.

As the $\text{HF}(v=1, J)$ rotational quantum number is increased from $J=0$ to $J=7$, two new bandheads appear, corresponding to the formation of $\text{CaF}(X^2\Sigma^+)$ in $v'=2$ and $v'=3$ (see fig. 1). In addition, the relative intensities of these heads grow as J increases.

4. Discussion

There have been relatively few experimental investigations of the role of reagent rotation in chemical reactions, and the majority of these concerned its effect upon the total reaction cross section [6–12]. Measurements of the partitioning of reagent rotation among product energy states have been reported for

Table 2

Reagent rotational quantum number dependence of relative product vibrational populations, $N_{v'}$, and average fraction of available energy appearing as vibration, $\langle f_{v'} \rangle$, for the reactions $\text{F} + \text{H}_2$ [14], $\text{Sr} + \text{HF}$ [15], and $\text{Ca} + \text{HF}$ (present work)

J	$N_{v'}$ d)						$\langle f_{v'} \rangle$
	$v'=0$	$v'=1$	$v'=2$	$v'=3$	$v'=4$	$v'=5$	
$\text{F} + \text{H}_2(v=0) \rightarrow \text{HF} + \text{H}^d)$							
0		0.25	1.00	0.56			0.70
1		0.30	1.00	0.47			0.67
2		0.27	1.00	0.63			0.69
$\text{Sr} + \text{HF}(v=1) \rightarrow \text{SrF} + \text{H}^b)$							
1	1.00	0.63	0.27	0.14	0.06	0.04	0.20
2	1.00	0.64	0.33	0.12	0.05	0.05	0.20
3	1.00	0.63	0.37	0.17	0.09	0.06	0.22
$\text{Ca} + \text{HF}(v=1) \rightarrow \text{CaF} + \text{H}^c)$							
0	1.00	0.55	0.21				0.18
1	1.00	0.56	0.22				0.18
2	1.00	0.58	0.24	0.03			0.19
3	1.00	0.60	0.28	0.05			0.20
4	1.00	0.65	0.33	0.10			0.21
5	1.00	0.71	0.39	0.15			0.21
6	1.00	0.78	0.47	0.22	0.05		0.23
7	1.00	0.82	0.56	0.30	0.11		0.24

a) Results are for a mass-weighted collision temperature of 290 K. The author also studied the reaction at a temperature estimated to lie between 100 and 200 K. Within the stated limits of error, there was no translational dependence of $N_{v'}$.

b) Values for $\langle f_{v'} \rangle$ are not reported in the original work. They are derived for the purposes of this table using the authors' stated experimental conditions and the spectroscopic constants from ref. [16].

c) In calculating $\langle f_{v'} \rangle$, spectroscopic constants from ref. [17] are employed.

d) Uncertainties for $N_{v'}$ are as follows: for $\text{F} + \text{H}_2$, ± 0.03 for $v'=1$ and 0.02 for $v'=3$; for $\text{Sr} + \text{HF}$, ± 0.02 . For $\text{Ca} + \text{HF}$ we estimate the error in $N_{v'}$ to be ± 0.10 for $J=0$ and $J=7$, and ± 0.05 for all other J values.

the reaction of F + H₂ [13,14]. An early study of the Sr + HF system by Karny et al. [3] showed intimations of efficient channeling of reagent rotation into product vibration. These observations were put on a more quantitative footing by Man and Estler [15]. The results for these two systems, as well as those for Ca + HF, are summarized in table 2. Both $N_{v'}$, the relative population of product vibrational level v' , and $\langle f_{v'} \rangle$, the average fraction of available energy appearing as product vibration, are presented. In the case of the present study, these quantities are derived from the data using a spectral simulation program. This simulation (see fig. 2) is carried out by assuming a distribution of rotational population (for each $N_{v'}$) given by

$$N_{J'}(v') \propto (2J' + 1)[E_{\text{tot}}(J) - E_{v'} - E_{J'}]^{1/2} \quad (2)$$

and by imposing an angular momentum cut-off at $J' = 73.5, 74.5$ ($N' = 74$). Here $E_{\text{tot}}(J)$ is the total energy available to the products when HF($v = 1$) is prepared in rotational state J , and $E_{v'}$ and $E_{J'}$ are the product vibrational and rotational energies. Vibrational populations are obtained by summing the $N_{J'}(v')$ over all J' . Aside from the angular momentum cut-off, this simulation corresponds to populating all energetically accessible levels in an egalitarian manner [18].

Values for $E_{\text{tot}}(J)$ (table 3) are obtained by treating this quantity as an adjustable parameter in the spectral simulation. In addition, $E_{\text{tot}}(J)$ is varied independently for only one value of J ; all other $E_{\text{tot}}(J)$ must scale as the HF rotational energy, i.e.

$$E_{\text{tot}}(J_1) - E_{\text{tot}}(J_2) = F(J_1) - F(J_2). \quad (3)$$

In this expression, J_1 and J_2 are arbitrary rotational quantum numbers for HF, and the $F(J)$ are the

Table 3

Total available energy and reagent rotational energy as a function of the HF($v = 1$) rotational quantum number. Units are kcal/mole

J	$E_{\text{tot}}(J)$	$E_{\text{rot}}^{\text{a)}$
0	5.05	0
1	5.16	0.11
2	5.39	0.34
3	5.73	0.68
4	6.18	1.13
5	6.75	1.70
6	7.43	2.38
7	8.22	3.17

^{a)} E_{rot} is the rotational energy of HF($v = 1$) [17].

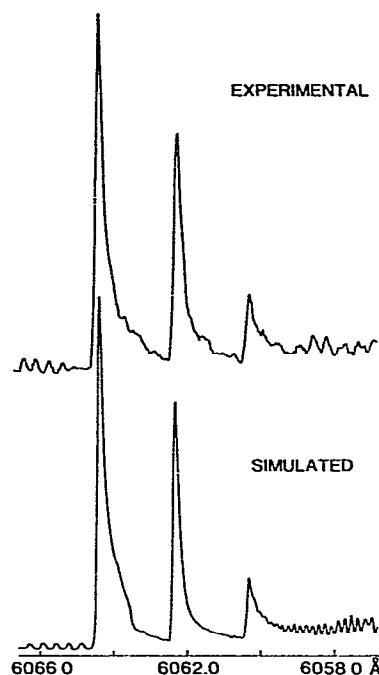


Fig. 2. Laser-excitation spectrum of CaF($A^2\Pi_{1/2} - X^2\Sigma^+$) for the reaction $\text{Ca} + \text{HF}(X^1\Sigma^+, v = 1, J = 3) \rightarrow \text{CaF}(X^2\Sigma^+, v', J') + \text{H}$, compared with computer simulation using the values of $N_{v'}$ given in table 3.

corresponding rotational term values. Thus one value of $E_{\text{tot}}(J)$ determines all the others. This quantity is then varied to achieve the best global fit for all values of the HF rotational quantum number.

The total energy can also be estimated from the reaction exoergicity and the collision energy:

$$E_{\text{tot}}(J) = E_{\text{int}}(J) + E_{\text{coll}}. \quad (4)$$

The collision energy in the center-of-mass frame, E_{coll} , is given by

$$E_{\text{coll}} = \frac{1}{2}\mu[3kT(\text{HF})/m(\text{HF}) + 4kT(\text{Ca})/m(\text{Ca})]. \quad (5)$$

Here, μ is the reduced mass of the collision partners and m , T , and k are, respectively, the mass, the temperature and the Boltzmann constant. The expression for the collision energy uses the root-mean-square relative velocity for a flux weighted beam and that for a gas in a bulb. Assuming HF and Ca temperatures of 300 and 1100 K, respectively, E_{coll} is 2.05 kcal/mole. The total internal energy of the reacting system, $E_{\text{int}}(J)$, is

$$E_{\text{int}}(J) = D_0^0(\text{CaF}) - D_0^0(\text{HF}) + E_{\text{int}}(\text{HF}, v = 1, J), \quad (6)$$

where $E_{\text{int}}(\text{HF}, \nu = 1, J)$ is the internal energy of reactant HF referred to $\text{HF}(\nu = 0, J = 0)$. Taking $D_0^0(\text{CaF}) = 127.1 \pm 2$ kcal/mole [19], $D_0^0(\text{HF}) = 135.1 \pm 0.3$ kcal/mole [20], and $E_{\text{int}}(\text{HF}, \nu = 1, J = 0) = 11.31$ kcal/mole [16], we obtain $E_{\text{tot}}(0) = 5.4$ kcal/mole, in agreement with the value in table 3 to well within the errors arising from the uncertainty in bond strengths and from our characterization of the distributions of $E_{\text{tot}}(J)$ as delta functions. The $\langle f_{\nu'} \rangle$ calculated using these $E_{\text{tot}}(J)$ are lower than those in table 2 by 5% of less.

The results in table 2 appear to delineate two substantially different types of reaction. For the highly exoergic reaction of F with H_2 ($E_{\text{tot}}(0) \approx 32$ kcal/mole), the non-statistical distribution of the $N_{\nu'}$, and the relatively large values of $\langle f_{\nu'} \rangle$ are characteristic of a process taking place upon a repulsive potential energy surface with "mixed energy release" [21]. There is also, apparently, a significant dynamical effect resulting from reagent rotation. It manifests itself as a suppression in product vibrational excitation when H_2 ($J = 1$, $E_{\text{rot}} = 0.34$ kcal/mole) is the reactant. In the present study, the maximum rotational energy introduced (3.2 kcal/mole) nearly equals the average energy available to the rotationless reagents (5.1 kcal/mole). The suitability of a nearly "unbiased" prior distribution for the spectral simulations suggest that the excess energy of reaction is being disposed statistically into all possible modes. As would be expected for a product distribution so characterized, the $N_{\nu'}$ decline monotonically with ν' and the $\langle f_{\nu'} \rangle$ approximate those calculated from a "vibrating-rotor" prior distribution [22]. Moreover Man and Estler [15] observe a similar pattern in their study of the homologous system, Sr + $\text{HF}(\nu = 1, J)$. The results of the present study are also in accord with the past success of phase space theory in predicting the dynamics for this class of reaction [23].

Acknowledgement

This work was supported in part by the National Science Foundation under Grant No. NSF-CHE-81-08823. We are grateful to the Center for Materials Research at Stanford for providing LiNbO_3 crystals for the OPO. We also thank David Yen for assistance in constructing the apparatus and Richard B. Bernstein for critically reading an earlier version of this manuscript.

References

- [1] J.C. Whitehead, in: Comprehensive chemical kinetics, Vol. 24, eds. C.H. Bamford and C.S.H. Tipper (Elsevier, Amsterdam, 1983) p. 357; M. Levy, Progr. Reaction Kinet. 10 (1979) 1.
- [2] T.J. Odiorne, P.R. Brooks and J.V.V. Kasper, J. Chem. Phys. 55 (1971) 1980; J.G. Pruett and R.N. Zare, J. Chem. Phys. 64 (1976) 1774; Z. Karny and R.N. Zare, J. Chem. Phys. 68 (1978) 3360; A. Torres-Filho and J.G. Pruett, J. Chem. Phys. 72 (1980) 6736; 77 (1982) 740.
- [3] Z. Karny, R.C. Estler and R.N. Zare, J. Chem. Phys. 69 (1978) 5199.
- [4] R.L. Herbst, R.N. Fleming and R.L. Byer, App. Phys. Letters 25 (1974) 520; S.J. Brosnan and R.L. Byer, IEEE J. Quantum Electron. QE-15 (1979) 415.
- [5] P.J. Dagdigian, H.W. Cruse and R.N. Zare, J. Chem. Phys. 60 (1974) 2330.
- [6] F.S. Klein and A. Persky, J. Chem. Phys. 61 (1974) 2472.
- [7] S. Stolte, A.E. Proctor, W.M. Pope and R.B. Bernstein, J. Chem. Phys. 66 (1977) 3468.
- [8] B.A. Blackwell, J.C. Polanyi and J.J. Sloan, Chem. Phys. 30 (1978) 299.
- [9] L. Zandee and R.B. Bernstein, J. Chem. Phys. 68 (1978) 3760.
- [10] B.A. Blackwell, J.C. Polanyi and J.J. Sloan, Chem. Phys. 24 (1977) 25.
- [11] H.H. Disper, M.W. Geis and P.R. Brooks, J. Chem. Phys. 70 (1979) 5317.
- [12] S.L. Anderson, P.R. Brooks, J.D. Fite and O.V. Nguyen, J. Chem. Phys. 72 (1980) 6521.
- [13] R.D. Coombe and G.C. Pimentel, J. Chem. Phys. 59 (1973) 1535.
- [14] D.J. Douglas and J.C. Polanyi, Chem. Phys. 16 (1976) 1.
- [15] C.-K. Man and R.C. Estler, J. Chem. Phys. 75 (1981) 2779.
- [16] K.P. Huber and G. Herzberg, Molecular spectra and molecular structures, Vol. 4. Constants of diatomic molecules (Van Nostrand, Princeton, 1979).
- [17] M. Dulick, P.F. Bernath and R.W. Field, Can. J. Phys. 58 (1980) 703.
- [18] R.B. Bernstein, Chemical dynamics via molecular beam and laser techniques (Oxford Univ. Press, London, 1982) pp. 205 ff.
- [19] Z. Karny and R.N. Zare, J. Chem. Phys. 68 (1978) 3360.
- [20] B. de B. Darwent, NSRDS-NBS 31 (1970).
- [21] J.C. Polanyi and J.L. Schreiber, Faraday Discussions Chem. Soc. 62 (1977) 267.
- [22] A. Ben-Shaul, R.D. Levine and R.B. Bernstein, J. Chem. Phys. 57 (1972) 5427.
- [23] A. Gupta, D.S. Perry and R.N. Zare, J. Chem. Phys. 72 (1980) 6237, 6259.